

# DOPPLER IMAGES OF THE PLEIADES ZAMS STARS HII 686 AND HII 3163

N. M. STOUT-BATALHA AND S. S. VOGT  
*UCO/Lick Observatory*  
*University of California*  
*Santa Cruz, CA 95064, U.S.A.*

## 1. Introduction

Of the steadily increasing number of Doppler Images appearing in the literature, the majority are of the RS CVn subclass of binary stars. The large rotational velocities and dynamo action of these stars is probably attributable to tidal spin-up of the active subgiant star by its binary companion. Their dynamos and resultant surface features (starspots) are thus almost certainly influenced by the companion. As such, these objects are not the ideal testing ground for comparison with single-star solar-like activity. Recently, a handful of Doppler images of single late-type main sequence and pre-main sequence stars have appeared in the literature. Pre-main sequence stars include V410 Tau (Joncour, Bertout, & Menard 1994), (Strassmeier, Welty, & Rice 1994), (Hatzes 1995) and HD 283572 (Joncour, Bertout, & Bouvier 1994). The main sequence stars include AB Dor (Collier Cameron & Unruh 1994), (Kürster, Schmitt, & Cutispoto 1994) and LQ Hya (Strassmeier, *et al.* 1993), (Saar & Piskunov 1994). These studies suggest that high-latitude dark spots are common to all rapidly-rotating stars, although, the spots found in the above work do not symmetrically *straddle* the pole as do polar spots of rapidly-rotating RS CVn binary stars.

As the sample of imaged stars grows, we will be able to study the onset and appearance of spots as a function of rotational period, and measure details about activity cycles and dynamo modes in both single and binary stars in different stages of evolution. Toward this end, we construct Doppler images of two rapidly-rotating, zero-age main sequence (ZAMS) stars in the Pleiades cluster: HII 686 (K5V) and HII 3163 (M0V). These very young stars are typically as faint as  $V=13$ . Image reconstruction of such faint, rapidly-rotating stars is not feasible on 3-m-class telescopes because an

observation long enough to provide the requisite S/N would result in considerable phase-smearing of the image. However, such objects are easily within the reach of the HIRES spectrograph on the Keck Ten-Meter Telescope. We used this facility during a HIRES commissioning night to obtain high resolution spectra of HII 686 and HII 3163. This paper presents the preliminary results of this work.

## 2. Observations

Our choice of target stars was based on the following criteria: (1) well-determined rotational period, (2) periodic photometric variability, (3) intermediate inclination angle, and (4) rotation period such that good phase coverage can be obtained in a single night's observations. The  $v \sin i$ , period, and assumed ZAMS radii were used to identify and avoid candidates with either high or low inclination angles. Table 1 lists the stars chosen and their relevant parameters, including our first guess at inclination angle.

TABLE 1. Program Stars

Object	$V$	$\Delta V$	$v \sin i$ [km/s]	Period [hrs] <sup>a</sup>	$i$ <sup>b</sup>	$T_{eff}$ [K]
HII 686	13.52	0.06	64	9.53	51° (42°)	4000
HII 3163	12.77	0.10	70	10.08	59° (30°)	4500

<sup>a</sup> from Van Leeuwen, Alphenaar, & Meys 1987

<sup>b</sup> first number is initial estimate; the number in parenthesis is the inclination (still preliminary) determined from the Doppler imaging analysis.

In December of 1993, high resolution ( $R = 67,000$ ) spectra of these objects were obtained at the Keck 10-meter telescope using the HIRES echelle spectrograph (Vogt et al. 1994). Seven observations of each star were taken at roughly hourly intervals through the course of one night (approximately 7.5 hours of observing). Because of the 10-hour rotational periods of these stars, we were able to obtain 70% phase coverage of both in a single night. Exposure times were fixed at 30 minutes so as to obtain adequate S/N while at the same time limiting phase smearing. Table 2 lists the observing log, calculated phases (zero epoch taken as midexposure of the first observation), and S/N (per pixel at  $\lambda 6430 \text{ \AA}$ ). During a 30-minute observation, each star rotated only about 18°. This 18° phase-smearing limits the size of the smallest resolvable features using the Fe I line. For the Ca I line, we are further limited in resolution by its broader intrinsic line width which allowed only about 4.2 resolution elements across the disk of HII 686 and 6.2 elements across HII 3163. We can thus expect to resolve only features larger than about 28° on HII 686 and 19° on HII 3163.

TABLE 2. Observing Log

Object	Date (UT) 12/18/93	$\Phi_{rot}$	S/N	Object	Date (UT) 12/18/93	$\Phi_{rot}$	S/N
HII 686	06:01:41	0.000	118	HII 3163	05:24:38	0.000	158
	07:07:19	0.115	117		06:34:18	0.115	157
	08:26:27	0.253	114		07:46:47	0.235	164
	09:33:18	0.370	111		08:59:08	0.355	163
	10:37:33	0.482	110		10:05:20	0.464	161
	11:44:55	0.600	101		11:09:34	0.570	137
	12:57:04	0.726	91		12:17:48	0.683	133

### 3. Spectral Synthesis

The process of Doppler image (DI) reconstruction requires knowledge of the shape and strength of specific intensity line profiles over the full range of limb angles in the un-spotted photosphere and, ideally, also in spotted regions. We use the grid of ATLAS9 model atmospheres computed by Kurucz (1992) to synthesize the relevant spectral region. We choose the region between  $\lambda 6425 \text{ \AA}$  and  $\lambda 6444 \text{ \AA}$  which includes both the Ca I  $\lambda 6439.075 \text{ \AA}$  line, (historically used in DI analyses), and the weaker Fe I line at  $\lambda 6430.844 \text{ \AA}$ . Other lines will be imaged in future work. To simplify computations, we assume that the shape and strength of the specific intensity profiles are the same in both the spotted and un-spotted regions. If this assumption were not valid, there would be variations in the disk-integrated equivalent width (EW) of the lines as a function of phase. We do not find any EW variations in these two lines which are larger than the intrinsic uncertainty in the measurements (5%).

The solar spectrum is used to establish realistic atomic line parameters. Because our program stars are significantly cooler than the Sun, we also observe and synthesize spectra of selected MK standard stars which have well-determined stellar parameters. We do this for the purpose of determining atomic line data for those lines which only become important at cooler temperatures. With the atomic data thereby established, the spectral region is synthesized using the model atmosphere which best represents each program star. For both objects, we assume a  $\log g$  of 4.5, solar abundances, a uniform microturbulence of  $2 \text{ km/s}$ , and  $T_{eff}$ 's as listed in Table 1. Figure 1 shows the phase-averaged observed line flux profiles (points) and disk-integrated rotationally-broadened synthesized profiles (lines) for both stars. Through the synthesis process, we are able to accurately determine the  $v \sin i$  of each star (Table 1). Then, using the above model atmosphere,

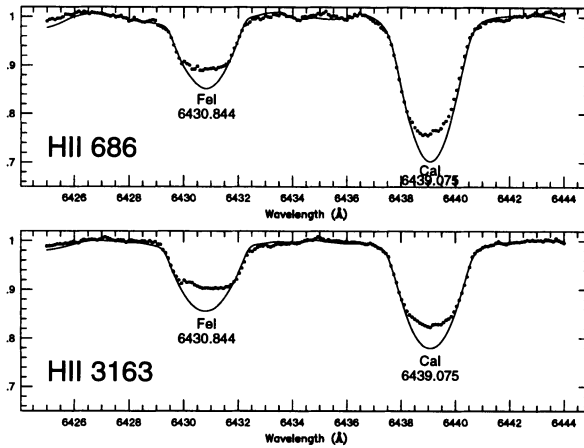


Figure 1. Spectral synthesis (solid) vs. observations (crosses)

we compute the local line profiles for a range of limb angles which well-sample the stellar disk. These specific intensity profiles are then input into the imaging code for the necessary line flux profile computations.

Note that the phase-averaged observed line flux profiles (points) in Figure 1 are considerably *flatter* in the core than the synthetic profiles (lines). This line core flattening is the classic signature of high latitude and/or polar spots and has often been criticized as stemming not from polar spots, but rather from an inability to properly synthesize line flux profiles from active stars. We share this concern and are studying the line synthesis problem in detail, quantifying the uncertainties by synthesizing profiles of standard stars. We will be including the effects of chromospheric emission and the effect of a chromosphere on the  $T(\tau)$  relation in the line-forming region. This work is in progress.

#### 4. Image Reconstruction

We use the maximum entropy Doppler imaging method described by Vogt, Penrod, & Hatzes 1987. Distortions due to spots as a function of phase are well-reproduced in both lines, and are also quite similar in many lines across the spectrum, showing that these spots are, to a very good approximation, ‘black’. Two other parameters necessary for image reconstruction are the star’s projected rotation velocity and the inclination. While the  $v \sin i$  is well-determined from the synthesis fitting procedure, the inclination angle is somewhat uncertain. Fortunately, Doppler image solutions are relatively insensitive to assumed inclination. Furthermore, the imaging procedure itself does provide a means to estimate inclination as both the goodness-of-fit of the final solution and the rate of convergence to the final solution de-

pend on how closely the assumed input inclination matches the true value. Preliminary values of  $42^\circ$  for HII 686 and  $30^\circ$  for HII 3163 were obtained in this way and are probably good to  $\pm 10^\circ$ , but the inclination determination is not yet finalized.

Figures 2 and 3 show respectively the resulting line fits and images for HII 686. Figures 4 and 5 show the same for HII 3163. The Doppler images are presented in flattened polar projection, down to a latitude of  $-45^\circ$ . The equator is shown by the bold latitude parallel. Observed phases are indicated by the short radial ticks around the periphery of each image. Also shown in Figures 2 and 4 are the residuals between the observations and the line fits. Residuals within the line profiles are consistent with the noise level of the data. No systematic residuals are found across the profiles, thereby assuring that the image is not under-fitting or over-fitting the line cores (which would produce either a spurious polar spot, or cause a real polar spot to disappear). In addition, the standard deviation of the residuals is not smaller than that of the noise in the observations, assuring that we are not over-fitting the data.

The images presented in Figures 3 and 5 are plotted using a gray-scale as opposed to a two-temperature intensity map. This makes it more difficult to discern spot boundaries, but does more fully display all of the information present in the solution. Images generated using the different lines are quite similar, though those from the Fe I lines contain more spatial structure as this intrinsically narrower line gives more resolution elements across the star.

## 5. Discussion

Our (preliminary) images reveal dark spots at very high latitudes on both ZAMS stars. HII 686 contains a prominent spot group (Figure 3) at about phase 0.1 and  $79^\circ$  latitude. In addition, images from both Fe I and Ca I of this star reveal several common features between  $5$  and  $55^\circ$  latitude. HII 3163 also shows prominent spots at high latitudes (Figure 5), but perhaps less evidence for spots at low-latitudes which are common to both the Fe I and the Ca I images. All of the spots on HII 3163 have latitudes between  $47$  and  $76^\circ$ . Interestingly, *neither* star shows a prominent axisymmetric spot straddling the pole, as is always seen on rapidly-rotating RS CVn stars. Furthermore, the high-latitude feature in the Fe I image of HII 3163 *may* have been resolved into a conglomeration of smaller features. Bear in mind that the observations of this star have larger S/N and this star also has more resolution elements across the stellar disk. We will be looking carefully into this question as imagery is derived from other lines.

The images presented herein represent only a 'first-pass' attempt at de-

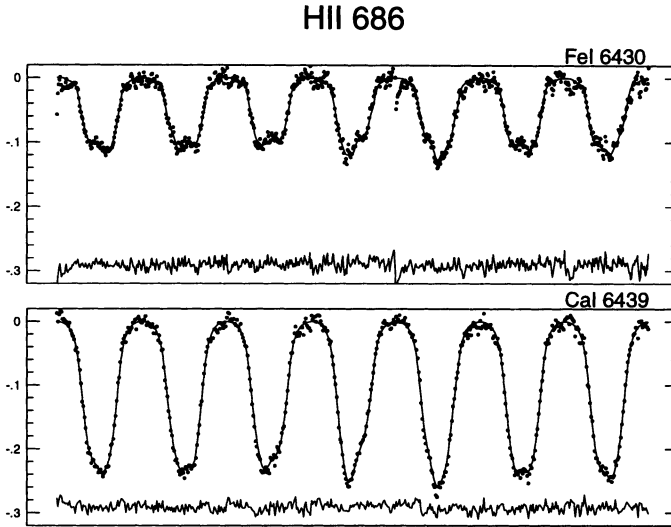


*Figure 2.* Observed flux profiles (points) and theoretical fits (line) for the Fe I phase-series (top) and Ca I phase-series (bottom) for HII 686. At the bottom of each graph are plotted the residuals of the data from the line fits.

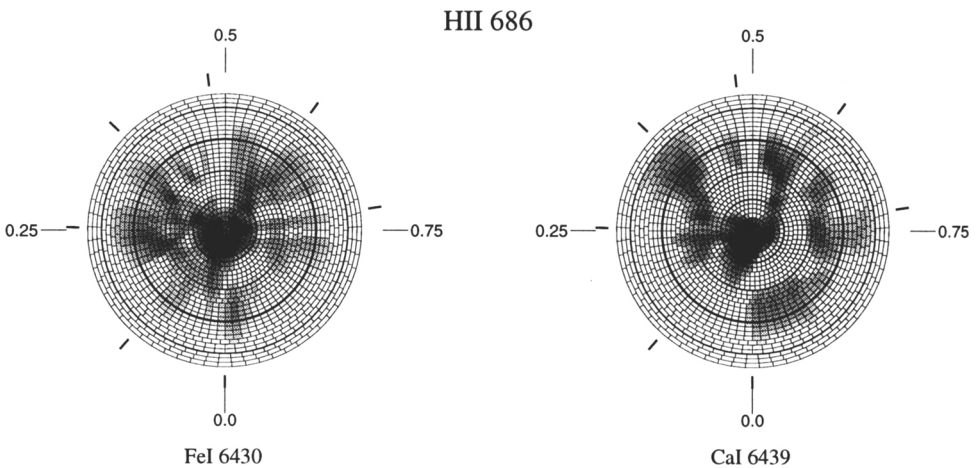


*Figure 3.* Doppler images of the M0V (ZAMS) star HII 686. These images are flattened polar projections which extend down to a latitude of  $-45^\circ$ . The equator is indicated by the bold latitude parallel.

ring Doppler images from our HIRES/Keck spectra, thus further analysis and discussion is unwarranted. They are presented primarily as an example of what is now achievable at  $V=13.5$  with a 10-m-class telescope. Because of their 10-hour rotation periods, quite short (30-minute) exposure times were used. Given the nod by a kind TAC, a single (queue-scheduled) 2-hour observation per night over a period of several days to several weeks would

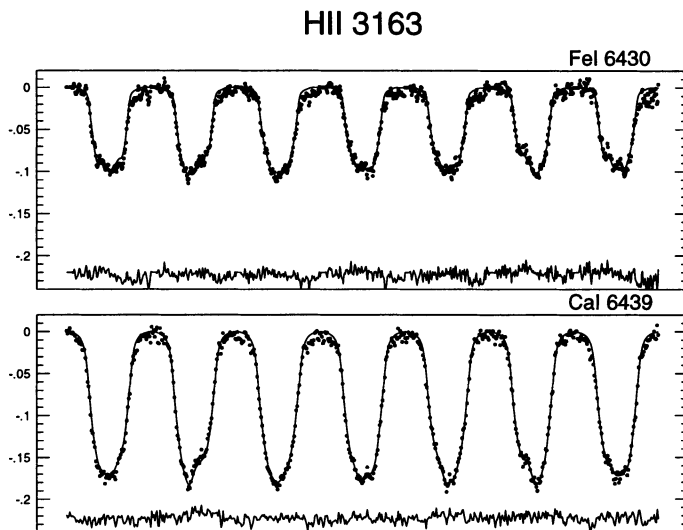


*Figure 4.* Observed flux profiles (points) and theoretical fits (line) for the Fe I phase-series (top) and Ca I phase-series (bottom) for HII 3163. At the bottom of each graph are plotted the residuals of the data from the line fits.

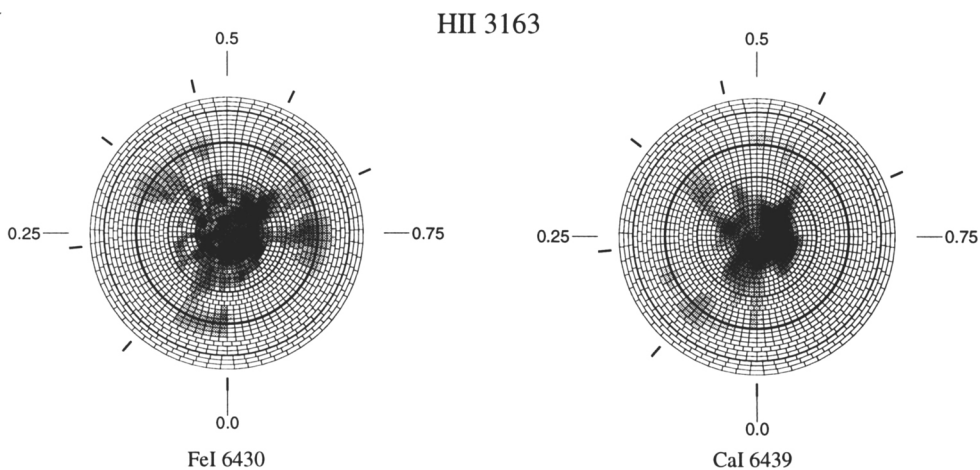


*Figure 5.* Doppler images of K5V (ZAMS) star HII 3163. These images are flattened polar projections which extend down to a latitude of  $-45^\circ$ . The equator is indicated by the bold latitude parallel.

allow a longer-period star as faint as  $V = 15$  to be easily Doppler imaged with the HIRES/Keck facility.



## 6. Future Work

Before any firm conclusions can be drawn from these images, we have more work to do in quantifying uncertainties in modeling line flux profiles of an un-spotted active star. We must also (1) add light curve constraints to our image solutions, (2) allow for the presence of hot spots in the imagery, (3) incorporate synthesis of asymmetric (i.e. blended) lines, and (4) incorporate temperature-sensitive line profile information (this requires lifting the assumption that the equivalent width in the spot and photosphere are the same). The HIRES echelle spectra include a host of other useful spectral lines, and we intend to derive images from many of these lines to better determine fine structure in the images, and to derive spot temperatures. Also of great interest are the chromospheric lines of H- $\alpha$ , and a Ca II infrared triplet line at  $\lambda 8498 \text{ \AA}$ . Both show large variations in equivalent width and (perhaps) periodic distortions in their profiles which will be possible to Doppler image. From such information, we expect to be able to ascertain the spatial relation between photospheric and chromospheric active regions.

In conclusion, we find evidence of prominent high-latitude (but not pole-straddling) cool spots on two rapidly-rotating ZAMS Pleiades stars. The dM0 star, HII 686, also shows evidence of low-latitude features while the dk5 star, HII 3613, largely does not. In addition, we *may* be resolving the high-latitude spot on HII 3613 into a conglomeration of smaller features.

## References

- Collier Cameron, A., Unruh, Y. C. 1994, *MNRAS*, **269**, 814.  
Hatzes, A. P. 1995, *ApJ*, submitted.  
Joncour, I., Bertout, C., and Bouvier, J. 1994, *A&A*, **291**, L19.  
Joncour, I., Bertout, C., Menard, F. 1994, *A&A*, **285**, L25.  
Kürster, M., Schmitt, J. H. M. M., Cutispoto, G. 1994, *A&A*, **289**, 899.  
Kurucz, R.L. 1992, in *The Stellar Populations of Galaxies*, IAU Symp. 149, eds. B. Barbuy & A. Renzini (Kluwer Acad. Pub.) 225.  
Saar, S. H., Piskunov, N. E. 1994, in *Proc. of the 8<sup>th</sup> Cambridge Workshop on Cool Stars, Stellar Systems, and the Sun*, Caillault, J. (ed.).  
Strassmeier, K. G., Rice, J. B., Wehlau, W. H., Hill, G. M., Matthews, J. M. 1993, *A&A*, **268**, 671.  
Strassmeier, K. G., Welty, A. D., Rice, J. B. 1994, *A&A*, **285**, L17.  
Vogt, S. S., Penrod, G. D., Hatzes, A. P. 1987, *ApJ*, **321**, 496.  
Vogt, S. S. *et al.* 1994 *S.P.I.E.*, **2198**, 362.  
Van Leeuwen, F., Alphenaar, P., Meys, J. J. M. 1987, *A&A Suppl.*, **67**, 483.